Environmental Science Nano

Accepted Manuscript

This is an *Accepted Manuscript*, which has been through the Royal Society of Chemistry peer review process and has been accepted for publication.

Accepted Manuscripts are published online shortly after acceptance, before technical editing, formatting and proof reading. Using this free service, authors can make their results available to the community, in citable form, before we publish the edited article. We will replace this *Accepted Manuscript* with the edited and formatted *Advance Article* as soon as it is available.

You can find more information about *Accepted Manuscripts* in the Information for Authors.

Please note that technical editing may introduce minor changes to the text and/or graphics, which may alter content. The journal's standard Terms & Conditions and the Ethical guidelines still apply. In no event shall the Royal Society of Chemistry be held responsible for any errors or omissions in this *Accepted Manuscript* or any consequences arising from the use of any information it contains.

ROYAL SOCIETY OF CHEMISTRY

rsc.li/es-nano

Nano impact statement

Assessing the health risk of exposure to nanoparticles is becoming increasingly important as nanoparticles are becoming more widely used in manufacturing and other realms employing nanotechnology. Additionally, it is of great importance to be able to collect useful data noninvasively. In this paper we demonstrate a novel cardiac health assessment method based on electrocardiogram recordings, which we show is sensitive to acute exposure events known to cause tissue damage, as observed in histological measurements. Our study represents a demonstration of the use of cardiac propagation stability as a powerful health assessment tool.

Environmental Science: Nano Accepted Manuscript

Journal Name

ARTICLE TYPE

Cite this: DOI: 10.1039/xxxxxxxxxx

Noninvasive evaluation of cardiac repolarization in mice exposed to single-wall carbon nanotubes and ceria nanoparticles via intratracheal instillation†

Karshak Kosaraju,[a] Jarrett L. Lancaster,*[a] Stephen R. Meier,[a] Steven Crawford,[a] Steven Hurley,[b] Shyam Aravamudhan[c] and Joseph M. Starobin[a]

Received Date
Accepted Date

DOI: 10.1039/xxxxxxxxxx

www.rsc.org/journalname

We present results obtained from electrocardiogram (ECG) measurements performed on mice exposed to single-walled carbon nanotubes and ceria nanoparticles through instillation. From these non-invasive ECG measurements, QT and RR intervals were obtained at various times after exposure and used to compute a novel metric for evaluating cardiac signal propagation stability, the reserve of refractoriness (RoR). It is demonstrated that while the isolated QT and RR intervals are essentially uncorrelated with histological data from hematoxylin and eosin stains of control and exposed tissue samples, the RoR is sensitive to cardiovascular effects from the exposure to nanoparticles.

1 Introduction

Carbon and metallic nanotubes have a great prospective for implementation in modern mechanics, electronics and medicine. However, the small size, large surface area and chemical reactivity of these nanostructures constitute a variety of essential environmental hazards.[1]

Recent experimental studies demonstrated even moderate pulmonary exposure to carbon nanotubes may trigger oxidative vascular damage which, in turn, may significantly accelerate the formation of atherosclerosis and atherosclerotic plaques.[2,3] It was also reported that acute exposure to ceria nanoparticles via inhalation may lead to cytotoxicity through oxidative stress response and ultimately lead to chronic inflammatory response with overloaded alveolar macrophages and neutrophils.[4] Although these findings conclusively demonstrated the importance of biochemical and immunological markers for identifying nanoparticle-induced oxidative stress and vascular damage, the association of such exposure with noninvasive electrophysiological factors is not understood. Even if monitoring of the cardiovascular system using electrophysiological measurements is one of the most robust biomedical tools, it is currently not adapted for applications in environmental toxicology. The development of non-invasive electrographic predictors of toxic effects on the human cardiovascular system is of a critical importance for public health and warrants aggressive exploratory research. Moreover, various studies have reported that both carbon nanotubes (CNTs) and ceria nanoparticles have demonstrated both pro- and anti-oxidative stress responses, thus making CNTs and ceria nanoparticles ideal candidates to study nanoparticle-related cardiotoxicity. The objective of the work is to study the effect of CNTs and ceria NPs on cardiac response, monitored non-invasively, in mice subjected to exposure via intra-tracheal instillation.

We employ the reserve of refractoriness (RoR) as a quantitative measure of stability for the acquired signals.[5] The analytically solvable, two-variable Chernyak-Starobin-Cohen (CSC) model[6] for electrical excitation of propagation in cardiac tissue allows one to compute the proximity of a given waveform to unstable regimes using only the QT and RR time intervals measured experimentally. The resulting measure of stability of propagating excitation known as the RoR, can be computed as discussed in the Supplementary Material. For each propagating excitation, there exists a critical value of the recovery current v_r^{crit}. If the recovery current cannot decrease below this value before the next excitation is initiated, stable propagation is not possible, and this one-dimensional mathematical instability corresponds to complex disruptions in the electrical activity on the two-dimensional cardiac surface. The CSC model parameters may be found from fitting computed QT and RR intervals to the values obtained from measured electrocardiogram (ECG) signals, allowing one to extract a prediction for v_r^{crit} as well as the actual minimum value attained by the recovery current, $v_{\min}$ (with $v_{\min} < v_r^{\text{crit}}$ for stable propaga-

[a] Department of Nanoscience, Joint School of Nanoscience and Nanoengineering, University of North Carolina at Greensboro, Greensboro, NC, USA. Fax: +1 336-500-0115; Tel: +1 336-285-2791; E-mail: jllancas@uncg.edu
[b] Department of Animal Sciences, North Carolina A&T State University, Greensboro, NC, USA.
[c] Department of Nanoengineering, Joint School of Nanoscience and Nanoengineering, North Carolina A&T State University, Greensboro, NC, USA.

† Electronic Supplementary Information (ESI) available: Mathematical details of reserve-of-refractoriness (RoR) calculations. See DOI: 10.1039/b000000x/

Environmental Science: Nano Accepted Manuscript

tion). The normalized difference between the critical value and the actual minimum constitutes the RoR. Previously, the *RoR* has been applied to ECG measurements collected from humans[5] and rats with and without spontaneous hypertensivity.[7] In this study, we will focus our attention on otherwise healthy mice exposed to carbon nanotubes and ceria nanoparticles.

2 Methods and Materials

2.1 Animals

A total of 30 female CD-1 mice 6-8 weeks of age (23.8 ± 2g) were purchased from Charles River Laboratories (Raleigh, NC). All mice were fed Purina 5001 –standard rodent chow– and provided water ad libitum throughout the study, and were weighed daily on an Arbor 1605 electronic balance. Mice were maintained in the laboratory animal research unit of North Carolina Agricultural and Technical State University. The protocol to perform ECG measurements and collect post-mortem samples was approved by the Institutional Animal Care and Use Committee (IACUC).

2.2 Nanoparticles

Preparation of SWCNTs dispersion: SWCNTs with 1-3 nm diameter and 1-2 μm length were purchased from Nanoamor, TX. The SWCNTs contained trace amounts of Co ($< 3\%$), Al ($< 0.1\%$), Cl ($< -.5\%$) and S ($< 0.3\%$). The nanotube dispersions were prepared by adding 4 mg (for low dosage) and 40 mg (for high doasage) of SWCNTs to 5 ml of phosphate buffered saline (PBS) followed by addition of 0.1% nonionic surfactant pluronic F68 (purchased from Sigma Aldrich, MO), to make a final concentration of 800 μg/mL and 8000 μg/mL for low and high dosages, respectively. The dispersions were sonicated for 2 hours. Ceria nanoparticle dispersion: Electrostatically stabilized, highly dispersed ceria NPs used in this study were obtained from Cabot Microelectronics. The ceria NPs, which are in the form of a model dispersion, are used for Chemical Mechanical Planarization (CMP) of wafers in semiconductor industry. The dispersion with pH of 3-4 was composed of 1% ceria NPs with diameter ranging from 60 to100 nm. The dispersion was diluted with PBS to make final concentrations of 400 μg/mL and 4000 μg/mL for low and high dosages, respectively.

2.3 Characterization

The nanoparticles were characterized for size by using a Carl Zeiss Libra 120 Plus transmission electron microscope (TEM) and vibrational information was obtained using a Horiba Xplora One Confocal Raman microscope. The nanoparticles were further characterized by dynamic light scattering (DLS) and zetasizer potential to measure volume-weighted hydrodynamic size distribution and zeta potential, respectively, using a Malvern Instruments ZEN 3600 Zetasizer Nano-ZX. Furthermore, the specific surface area of ceria NPs was measured using a Nova Quantachrome 2200e BET surface area analyzer.

2.4 ECG measurements

The instrument used for noninvasive ECG measurement in conscious, CD-1 mice was ECGenie ECG recording platform Mouse Specific, Inc, MA (Fig. 1). The ECGenie was installed on-site with technical support from Mouse Specifics. The software for data acquisition (LabChart7) and data analysis (Mouse) were installed on a Dell Latitude laptop with an Intel Core i7 processor. Equipment was tested and baseline parameter optimization was performed with an initial set of conscious mice.

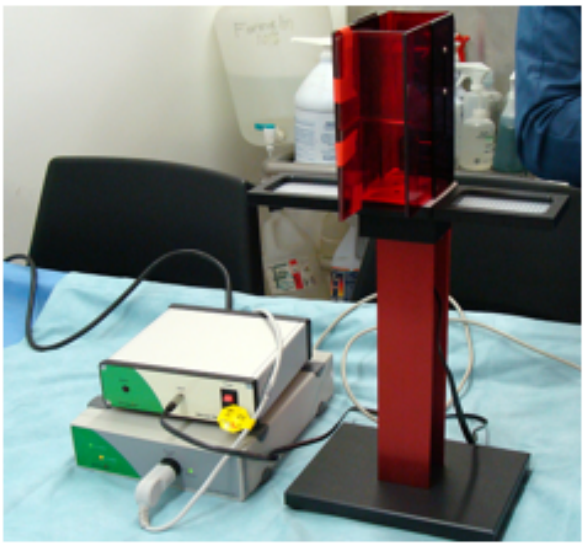

Fig. 1 ECGenie system with electronics, including a chamber and platforms for ECG measurements.

All mice were ear tagged and weighed immediately upon arrival to the animal facility. One day was determined to be sufficient for acclimatization of mice to the ECGenie system to allow reliable data recording. The mice were randomly assigned to control ($n = 5$), low dosage ($n = 5$), and high dosage ($n = 5$) groups for SWCNT and ceria NP exposure. Pre-exposure ECG signals were recorded for all groups. After the pre-exposure measurement, lightly anaesthetized animals were exposed via intratracheal instillation to either SWCNTs dispersed in 50 μL PBS or ceria NPs in model ceria CMP slurries. Following nanoparticle instillation, ECG recordings were performed in all groups of mice on days one and three, respectively. An additional measurement was performed for the groups exposed to SWCNT at the seventh day after exposure. After completion of ECG recordings all mice were euthanized with isoflorane followed by cardiac puncture to collect blood, lungs, trachea and heart for ex vivo analyses. Post-mortem 0.5-1 mL blood samples were collected to evaluate blood lactate dehydrogenase (LDH) and differential cell counts to assess toxicity of exposure. Organs of the mice (trachea, lungs, heart) were harvested and stored at -80°C for immunohistology and ultrastructural characterization.

2.5 Acquisition of QT/RR intervals

Segments of signals containing at least six distinguishable waveforms were processed using ECGenie software, resulting in indi-

Environmental Science: Nano Accepted Manuscript

This journal is © The Royal Society of Chemistry [year]

vidual *QT* and *RR* measurements for each waveform. To obtain a single pair of *QT* and *RR* intervals for each measurement event, the numerous values for each measurement event were averaged. Within each measurement event, *QT* and *RR* values differing by more than 2.7 standard deviations from the mean were classified as outliers and excluded from the subsequent analysis.

2.6 RoR Calculation

A pair of average *QT* and *RR* intervals for each mouse at each measurement event was used to fit the measured signal to the CSC model. Mathematical details of the model and the fitting procedure are discussed in the supplemental material.†One of the fitting parameters corresponds to the minimum value attained by the CSC recovery current, $v_{\min}$. The critical recovery current v_r^{crit} was computed from the remaining parameters, and the *RoR* followed from the normalized difference between these two quantities as:

$$RoR = \frac{v_r^{\text{crit}} - v_{\min}}{v_r^{\text{crit}}}. \quad (1)$$

Statistical analyses were performed using MedCalc for Windows, version 12.5 (MedCalc Software, Ostend, Belgium).

3 Results

3.1 Characterization of SWCNTs

The CNT dispersions were characterized using TEM and Confocal Raman Microscopy. Fig. 2(a) shows transmission electron microscope (TEM) image which indicates a good dispersion of SWCNTs. Using Malvern Zetasizer the SWCNTs were also characterized for volume-weighted hydrodynamic size and dispersibility by using DLS and zeta potential measurements, respectively. Before dispersing, the SWCNTs had a volume-weighted hydrodynamic size of 2242 d.nm and a zeta potential of -49.8mV in water, which changed to 227 d.nm and -21.4 mV, respectively, after dispersing in pluronic F68. We note that DLS measurements do not produce valid data for SWCNTs because of their non-spherical nature. However, these measurements, along with zeta potential measurements, are useful for monitoring the CNT dispersibility in the presence of surfactants. The SWCNTs were also further characterized in a Horiba Confocal Raman Microscope. Raman spectra of SWCNTs (Fig. 2(b) indicate the presence of radial breathing mode, D, G and G' bands, which verifies SWCNTs in the dispersion.

3.2 Characterization of ceria nanoparticles

Nitrogen adsorption-desorption isotherms were collected for dried ceria NPs and specific surface area of 16.979 m^2/g was determined using extension of Langmuir Theory. Fig. 2(c) shows TEM image of dried ceria NPs which indeed indicates that the diameter of the NPs is in the range of 74 ± 16 nm confirming the diameter obtained from the manufacturer. The ceria nanoparticles were characterized by DLS which indicated the volume-weighted hydrodynamic size distribution of 145.3 ± 2.6d.nm when diluted 100x in water and zeta potential measurements, which indicated the surface charge to be 42.7 ± 1.4mV. The ceria nanoparticles were further characterized using a Horiba Confocal Raman Microscope. Raman spectrum of SWCNTs (Fig. 2(d)) indicates the presence of Ce-O vibrational band at 450 cm^{-1}.

3.3 RoR measurements

The *RoR* was computed for each mouse at each measurement event on each day. The *QT*/*RR* interval average values and standard deviations over an entire day for the mice with median number of usable waveforms are shown in Table 1. The term "usable waveform" refers to action potential events which could be clearly identified from the ECG measurements and were not excluded as outliers, as discussed above. Results of exposure to SWCNTs demonstrate a more significant effect in the high dosage mice compared to the low-dosage group, as depicted in the box plots in Fig. 3 and Table 2. The mice exposed to the low dosage of SWCNTs demonstrated positive trends in *RoR* change, whereas the mice treated with high dosage of SWCNTs showed negative trends in *RoR*. That is, *RoR* measurements decreased in the mice exposed to the higher dosage while appearing to increase for mice exposed to the lower dosage. It should be noted that the low-dosage group's trend showed little significance ($p > 0.3$), whereas the high-dosage group's trend possessed marginal ($p > 0.054$) significance (Table 2). Interestingly, the corresponding *RR* and *QT* interval measurements appear largely uncorrelated with *RoR*, and consequently uncorrelated with the evidence of cardiac toxicity uncovered through tissue analysis (see next section). Unlike the mice exposed to SWCNTs, both groups exposed to ceria (high and low dosages) exhibited a drop in *RoR* over time (Fig. 4, Table 3). Interestingly, the *RoR* dipped by 1.4% from its initial (pre-exposure) Day 0 value after one day and then by more than 6% (also compared to Day 0) on Day 3 for the low-dosage group with marginal significance ($p = 0.064$). The group exposed to a high dosage of ceria exhibited the opposite behavior, with an initial drop in RoR by 4.29% on Day 1, followed by a slight recovery with RoR on Day 3, being only 2.65% below the pre-exposure value. For this high-dosage group, marginal significance was observed only for the 4.% drop on Day 1 ($p = 0.074$).

3.4 Tissue Analysis

Fig. 5(a) shows healthy (control) lung tissue which has a good spacing in the alveoli, bronchioles and alveolar ducts. Figures 5(b) and (c) show images of lung tissue in mice exposed to low and high dosages of SWCNTs, respectively. It can be observed that the space in the alveoli and the alveolar ducts are infiltrated with cells as a consequence of inflammatory response. This effect is significant (Fig. 5(c)) in mice treated with high dosage of SWCNTs, and minimal (Fig. 5(b)) in mice treated with low dosage of SWCNTs. Figs. 5(d) and (e) show images of lung tissue of mice exposed to low and high dosages of ceria NPs, respectively. In this case the alveolar spacing decreases significantly even in mice exposed to low dosage of ceria NPs resulting in constriction of bronchiole (Fig. 5(d)). The trend becomes stronger indicating the deterioration of lung tissue, whereas mice treated with high dosage of ceria NPs expose large areas of collapsed bronchioles (Fig. 5(e)) indicating severe damage to the lung tissue. In

Environmental Science: Nano Accepted Manuscript

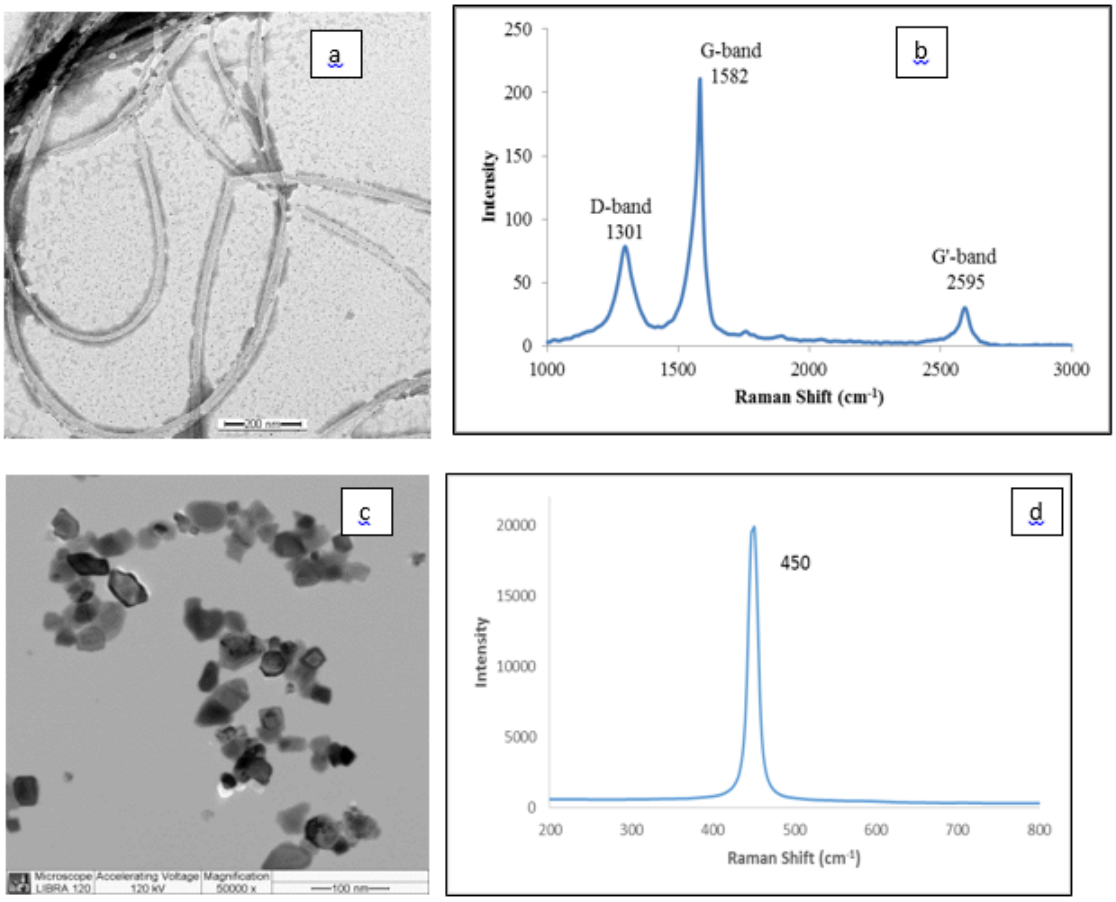

Fig. 2 (a) TEM image of SWCNTs dispersed in 1% pluronic F68; (b) Plot shows Raman spectrum of SWCNTs which indicates the presence of radial breathing mode, D, G and G' bands typical for carbon nanotubes; (c) TEM image of ceria NPs; (d) Raman spectrum of ceria NPs which indicates the presence of a characteristic peak at 450 cm^{-1}.

Table 1 *RR* and *QT* averages with standard deviations for mice in each group corresponding to the median number of processed waveforms within each group. Groups consisted of Control (zero dose), Low and High doses of CNT/Ceria nanoparticles across all days.

Group	Mouse	Day	Num. Waveforms	*RR*(ms)	*RR* std. dev. (ms)	*QT*(ms)	*QT* std. dev. (ms)
SWCNT-C	1	3	229	83.5	7.11	41.5	8.16
SWCNT-L	8	3	384	84.4	5.46	41.4	8.06
SWCNT-H	12	7	276	76.0	3.41	39.4	6.44
Ceria-C	17	3	193	75.1	3.25	38.2	8.10
Ceria-L	22	3	242	76.7	3.31	39.9	6.14
Ceria-H	30	1	370	81.3	7.26	41.9	7.79

Table 2 Percentage change in *RoR* for SWCNT exposure from day zero for low- and high-dose groups on various days shown with *p*-values. *RR* and *QT* interval measurements are also shown for comparison.

Group	*RoR*% Change from Day 0	*p*-value	*RR*% Change from Day 0	*p*-value	*QT*% Change from Day 0	*p*-value
Day 1 Low	+2.23	0.6044	-7.12	0.1121	-8.62	0.0209
Day 3 Low	+3.89	0.3181	-0.05	0.9867	-2.00	0.4594
Day 7 Low	+1.23	0.6915	-1.90	0.5068	-2.62	0.1660
Day 1 High	-7.29	0.0829	-7.22	0.1112	-2.80	0.5224
Day 3 High	-4.37	0.1159	-6.81	0.0959	-3.76	0.4674
Day 7 High	-5.29	0.0540	-9.21	0.1345	-5.32	0.2414

Table 3 Percentage change in *RoR* for ceria NP exposure from day zero for low- and high-dose groups on various days shown with *p*-values. *RR* and *QT* interval measurements are also shown for comparison.

Group	*RoR*% Change from Day 0	*p*-value	*RR*% Change from Day 0	*p*-value	*QT*% Change from Day 0	*p*-value
Day 1 Low	-1.4	0.7321	+0.86	0.8565	+0.54	0.8499
Day 3 Low	-6.3	0.0642	-6.30	0.0002	-2.26	0.3485
Day 1 High	-4.29	0.0740	-1.67	0.5364	+1.04	0.7095
Day 3 High	-2.65	0.2666	+1.21	0.7858	+2.93	0.4999

Environmental Science: Nano Accepted Manuscript

This journal is © The Royal Society of Chemistry [year]

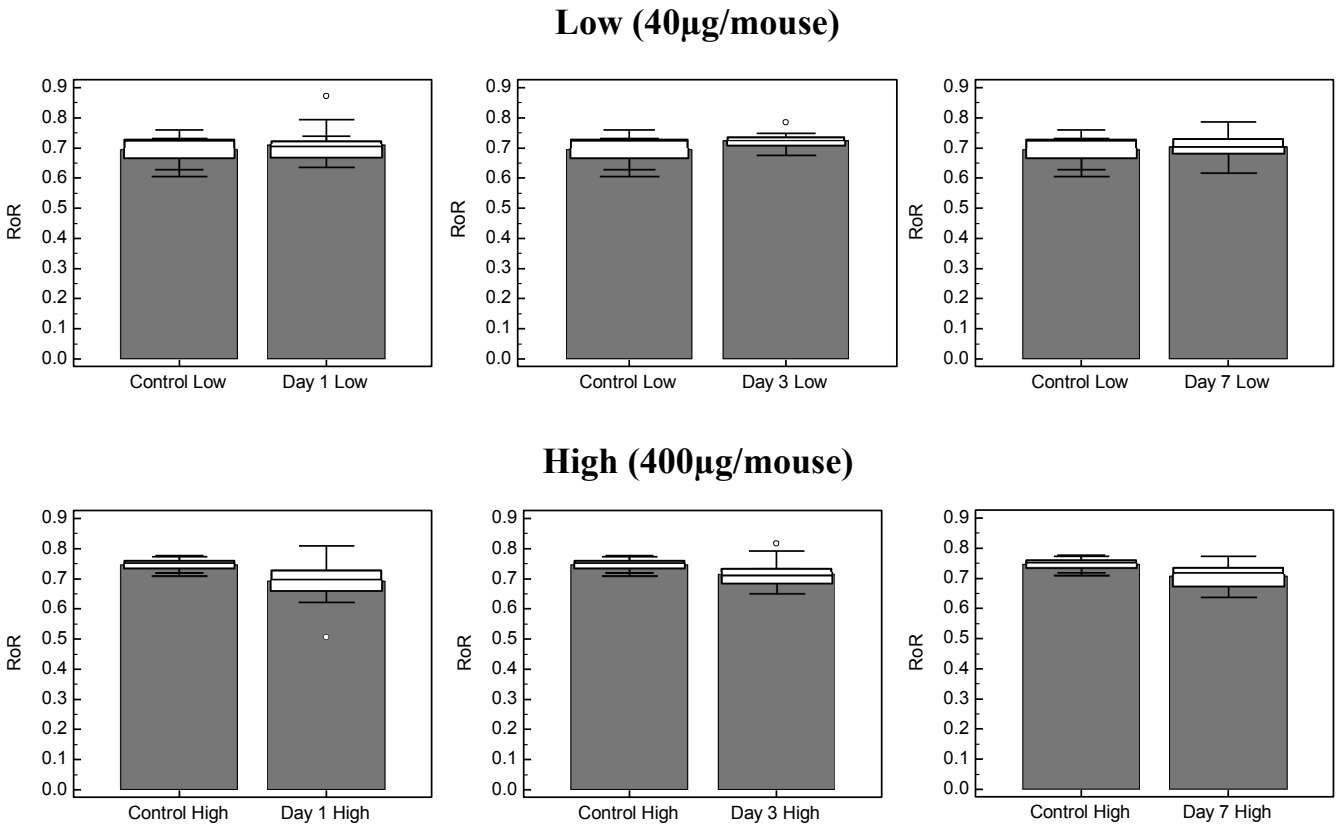

Fig. 3 Box-plot comparison of control (Day 0) and post-exposure *RoR* values for mice exposed to SWCNTs. Each boxplot represents a comparison of five measurements on Day 0 to 20 measurements of the same five mice on subsequent days after exposure.

summary, even though none of the mice died over seven day observation period, we noticed distinct lung tissue damage which was enhanced at higher dosages of nanoparticles. It should be also emphasized that a stronger dosage effect was found for ceria nanoparticles which was in a good agreement with observed dynamics of *RoR*.

4 Discussion

With increasing usage of nanoparticles in modern industry, understanding the adverse effects of nanoparticles on cellular systems and organs is of extreme importance. SWCNTs and ceria nanoparticles are two types of nanoparticles which have been extensively studied for use in various applications including manufacture of commercial products and drug delivery. Therefore, it is important to study the effect of these nanoparticles on living systems. Although many studies have reported effects of nanoparticles on several cell types in vitro and several organs in vivo, there is minimal understanding regarding the effects of nanoparticles on the heart. Even though there are robust invasive techniques to study, measure and evaluate the functioning of the heart, there is an urgent need to collect these measurements noninvasively. In this study, we employ a novel method that uses QT and RR intervals from a surface electrocardiogram, to predict cardiac toxicity in mice exposed to SWCNTs and ceria NPs.

Recent findings demonstrate that exposure to carbon and metallic nanoparticles can cause cytotoxic effects in vascular endothelial cells.[2,8,9] Yan *et al* reported that pulmonary exposure to SWCNTs may induce cardiovascular toxicity via indirect effects on vascular homeostasis.[10] It has been reported that instillation of SWCNTs with a diameter of 1-2 nm and length of up to 100 um in mice[11] and rats[12] could lead to the formation of lung granuloma. Recent reports provide evidence that exposure to ceria NPs causes adverse effects in various organs including lungs, liver, spleen, kidneys, brain and heart, as well as their related cellular systems.[13] Supporting the antioxidant nature of ceria nanoparticles, Pagliari et al reported that 24 hour exposure to ceria nanoparticles did not affect cell growth and function while protecting from H_2O_2-induced cytotoxicity for at least 7 days in cardiac progenitor cells.[14] However, another study by Poma et al demonstrates inflammatory response with no lethal toxic effects in CD-1 mice exposed to cerial NPs through oral administration, suggesting that ceria NPs are not completely safe.[15] These findings show that cardiovascular effects due to nanoparticle exposure occur mainly through systemic inflammatory cascades, which can potentially lead to abnormal electrophysiological response in the heart.

Our observations based on the dynamics of *RoR* show that ceria nanoparticles induce greater toxicity and tissue damage compared to the SWCNTs used in this study. Concurrently, it was found that there was more tissue damage in case of mice exposed to ceria NPs. The mice treated with low concentration of SWCNTs did not show significant damage, but the mice treated with the high dosage of the same SWCNTs showed tissue damage with

Environmental Science: Nano Accepted Manuscript

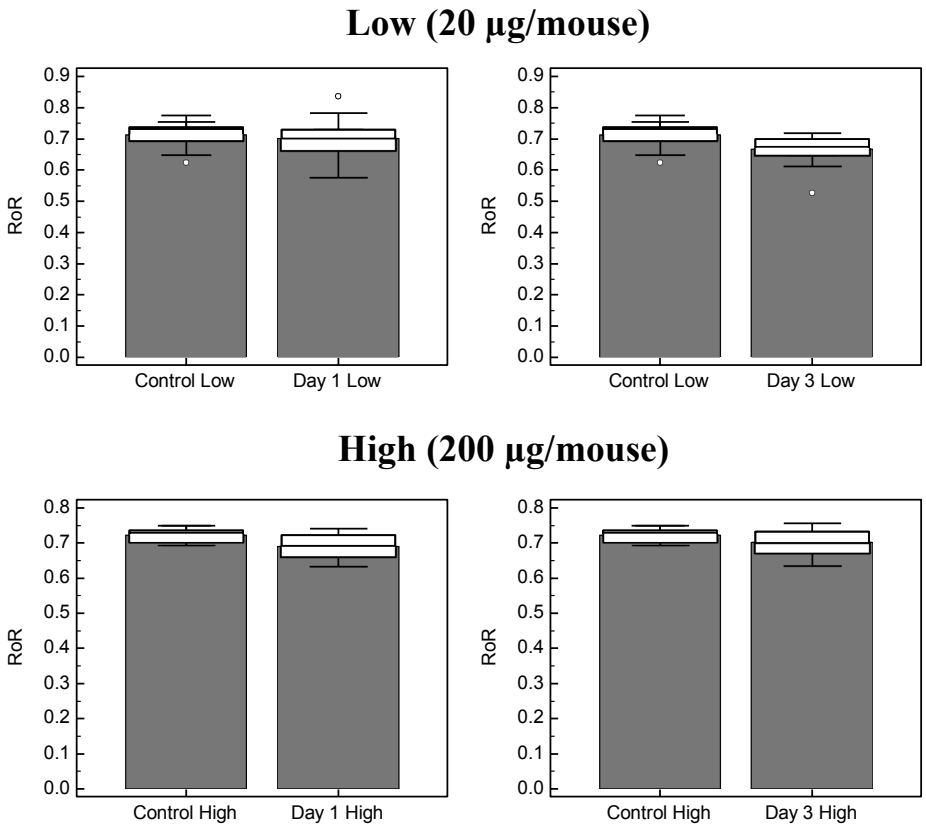

Fig. 4 Box-plot comparison of control (Day 0) and post-exposure *RoR* values for mice exposed to ceria NP. Each boxplot represents a comparison of five measurements on Day 0 to 20 measurements of the same five mice on subsequent days after exposure.

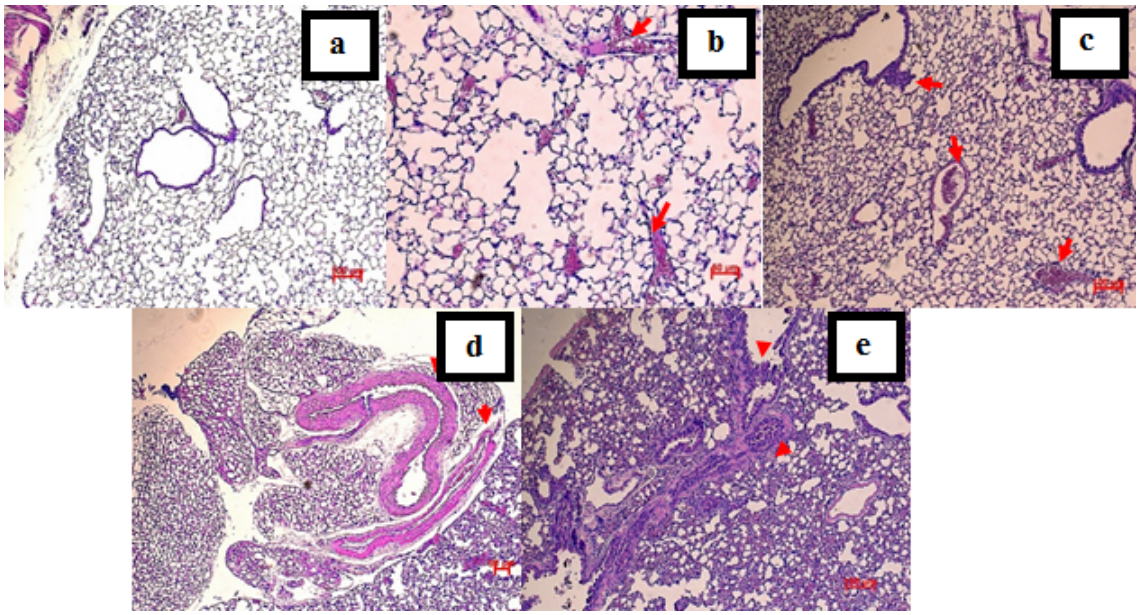

Fig. 5 Hematoxylin and Eosin (H&E) stains of lung tissues in control mouse (a) and mice exposed to SWCNTs and ceria NPs (b)-(e): Control (a); Low-dosage SWCNTs (b); High-dosage SWCNTs (c); Low-dosage ceria NPs (d); High-dosage ceria NPs (e).

Environmental Science: Nano Accepted Manuscript

This journal is © The Royal Society of Chemistry [year]

less alveolar air space, infiltration of immune cells and formation of septa. The lung tissue damage was found to increase with concentration in case of both SWCNTs and ceria instilled CD-1 mice. However, similarly to the mice exposed to a high dosage, the low dosage of ceria also caused lung tissue damage with shortening of bronchiolar space and infiltration of immune cells. However, the effects were comparatively severe in case of mice instilled with high dosage of ceria where collapse of bronchi was also observed.

Even though the *RoR* values showed trends indicative of cardiotoxicity due to SWCNTs and ceria nanoparticles in agreement the histological analysis, the *p*-values were marginal. However, even marginal trends in the *RR* and *QT* intervals were absent, strongly suggesting that information relevant to cardiac toxicity was absent from these isolated measurements. The *RoR* constitutes a legitimate measure of refractoriness which is statistically independent of the *RR* and *QT* intervals and highly sensitive to cardiac toxicity. Furthermore, by fitting each ECG signal to the CSC model for electrical signal propagation in cardiac tissue and obtaining a measure of the reserve of refractoriness (see Supplementary Material), our approach takes into account the individualized stability thresholds of each subject. This personalized aspect to the *RoR* allows for sensitivity to minor changes due to acute toxicity, as observed here. Common risk factors for serious cardiovascular events (i.e., myocardial infarctions) such as the numerous "corrected" *QT* intervals are empirical in nature, only meaningful as statistical markers which can effectively separate severe disease cases from normal healthy behavior.[16]

Since toxic cardiac responses such as arrhythmias and ischemia should depend on levels of physiological load, it is desirable to perform the measurements under dobutamine-induced cardiac stress. As explored by Hazari *et al*,[17] dobutamine causes the heart to respond as if the animals were exercising in a conventional "stress" test. When exposed to diesel exhaust, spontaneously hypertensive rats show a drop in heart-rate variability compared to otherwise healthy rats which becomes more significant when dobutamine is used to simulate a stress test. The *RoR* provides a concise metric, complimentary to heart-rate variability, which has recently been demonstrated to be sensitive to the effects of spontaneous hypertensivity in the presence of diesel exhaust. Specifically, spontaneously hypertensive rats exposed to diesel exhaust show a more severe drop in *RoR* with increasing dobutamine dosages compared to otherwise healthy animals.[7] Consequently, one direction for future research currently being explored is to consider several classes of mice with varying states of predisposition to disease. By exposing these different groups to a variety of nanoparticles and subjecting them to dobutamine stress tests, the role of pre-existing conditions during exposure may be investigated.

5 Acknowledgments

This work was supported by NSF-CBET (award number 1342051).

References

1 G. L. Hornyak, H. F. Tibbals, J. Dutta and J. J. Moore, *International Technology Roadmap for Semiconductors*, CRC Press, Boca Raton, FL, USA, 2009.

2 Z. Li, T. Hulderman, R. Salmen, R. Chapman, S. S. Leonard, S.-H. Young, A. Shvedova, M. I. Luster and P. P. Simeonova, *Environ. Health Perspect.*, 2007, **115**, 377–382.

3 P. Stenvinkel, *Nephrol. Dial. Transplant.*, 2001, **16**, 1968–1971.

4 A. Srinivas, P. J. Rao, G. Selvam, P. B. Murthy and P. N. Reddy, *Toxicol. Lett.*, 2011, **205**, 105–115.

5 S. F. Idriss, W. K. Neu, V. Varadarajan, T. Antonijevic, S. S. Gilani and J. M. Starobin, *Computing in Cardiology*, 2012, **39**, 353–356.

6 Y. B. Chernyak, J. M. Starobin and R. J. Cohen, *Phys. Rev. Lett.*, 1998, **80**, 5675–5678.

7 M. S. Hazari, J. L. Lancaster, J. M. Starobin, A. K. Farraj and W. E. Cascio, *Cardiovascular Toxicology*, 2016, 1–10.

8 A. Gojova, B. Guo, R. S. Kota, J. C. Rutledge, I. M. Kennedy and A. I. Barakat, *Environ. Health Perspect.*, 2007, **115**, 403–409.

9 J. Sun, S. Wang, D. Zhao, F. H. Hun, L. Weng and H. Liu, *Cell Biology and Toxicology*, 2011, **27**, 333–342.

10 J. Yan, Z. Lin, B. Lin, H. Yang, W. Zhang, L. Tian, H. Liu, H. Zhang, X. Liu and Z. Xi, *Toxicol Res.*, 2015, **4**, 1225–1237.

11 C.-W. Lam, J. T. James, R. McCluskey and R. L. Hunter, *Toxicol. Sci.*, 2004, **77**, 126–134.

12 D. B. Warheit, B. R. Laurence, K. L. Reed, D. H. Roach, G. A. M. Reynolds and T. R. Webb, *Toxicol. Sci.*, 2004, **77**, 117–125.

13 L. Geraets, A. G. Oomen, J. D. Schroeter, V. A. Coleman and F. R. Cassee, *Toxicol. Sci.*, 2012, **172**, 463–473.

14 F. Pagliari, C. Mandoli, G. Forte, E. Magnani, S. Pagliari, G. Nardone, S. Licoccia, M. Minieri, P. D. Nardo and E. Traversa, *Am. Chem. Soc. Nano*, 2012, **6**, 3767–3775.

15 A. Poma, A. M. Ragnelli, J. de Lapuente, D. Ramos, M. Borras, P. Aimola, M. D. Gioacchino, S. Santucci and L. D. Marzi, *J. Immunol. Res.*, 2014, **2014**, 361419.

16 J. M. Dekker, R. S. Crow, P. J. Hannan, E. G. Schouten and A. R. Folsom, *JAAC*, 2004, 565–571.

17 M. S. Hazari, J. Callaway, D. W. Winsett, C. Lamb, N. Haykal-Coats, Q. T. Krantz, C. King, D. L. Costa and A. K. Farraj, *Environ. Health Perspect.*, 2012, **120**, 1088–1093.

Environmental Science: Nano Accepted Manuscript